MDPI

Article

Pt/WO$_3$ Nanoparticle-Dispersed Polydimethylsiloxane Membranes for Transparent and Flexible Hydrogen Gas Leakage Sensors

Ryo Ishihara [1,†] , Yoshihiro Makino [1,†] , Yuki Yamaguchi [2] , Kenjiro Fujimoto [2] and Keishi Nishio [1,*]

1   Department of Materials Science and Technology, Tokyo University of Science, 6-3-1 Niijuku, Katsushika, Tokyo 125-8585, Japan; r-ishihara@juntendo.ac.jp (R.I.); 8216656@alumni.tus.ac.jp (Y.M.)
2   Department of Pure and Applied Chemistry, Tokyo University of Science, Noda 278-8510, Japan; y-yamaguchi@aist.go.jp (Y.Y.); fujimoto_kenjiro@rs.tus.ac.jp (K.F.)
*   Correspondence: k-nishio@rs.tus.ac.jp
†   These authors contributed equally to this work.

Abstract: Hydrogen gas is a promising, clean, and highly efficient energy source. However, to use combustible H$_2$ gas safety, high-performance and safe gas leakage sensors are required. In this study, transparent and flexible platinum-catalyst-loaded tungsten trioxide (Pt/WO$_3$) nanoparticle-dispersed membranes were prepared as H$_2$ gas leakage sensors. The nanoparticle-dispersed membrane with a Pt:W compositional ratio of 1:13 was transparent and exhibited a sufficient color change in response to H$_2$ gas. The membrane containing 0.75 wt.% of Pt/WO$_3$ nanoparticles exhibited high transparency over a wide wavelength range and the largest transmittance change in response to H$_2$ gas among the others. The heat treatment of the particles at 573 K provided sufficient crystallinity and an accessible area for a gasochromic reaction, resulting in a rapid and sensitive response to the presence of H$_2$ gas. The lower limit of detection of the optimized Pt/WO$_3$ nanoparticle-dispersed membrane by naked eye was 0.4%, which was one-tenth of the minimum explosive concentration. This novel membrane was transparent as well as flexible and exhibited a clear and rapid color response to H$_2$. Therefore, it is an ideal candidate sensor for the safe and easy detection of H$_2$ gas leakage.

Keywords: hydrogen gas sensor; polydimethylsiloxane; transparent; flexible; platinum-catalyst-loaded tungsten trioxide

1. Introduction

Hydrogen gas is expected to emerge as a next-generation energy source because of its high energy density and low environmental load compared with fossil fuels [1]. However, it is a transparent and odorless gas that poses a risk of explosion when its concentration in the atmosphere is in the approximate range of 4–74 vol%. In addition, hydrogen has a relatively high diffusion coefficient compared with other combustible gases. Therefore, gas leakage detection sensors are essential for its safe utilization. Current semiconductor-type and contact combustion-type hydrogen sensors have a disadvantage of requiring high operating temperatures and heating processes. They cannot be used when power failures occur because a power supply would be required to detect the changes in the electrical resistance of the elements. Moreover, it is desirable that the sensors can be used for leakage detection in transportation pipes and storage tanks with complicated shapes.

Platinum-loaded tungsten trioxide (Pt/WO$_3$) exhibits a rapid and reversible color change (known as gasochromism) through redox reactions with hydrogen and oxygen, even at room temperature [2–4]. The gasochromism of Pt/WO$_3$ consists of four steps: (i) decomposition of hydrogen molecules to hydrogen atoms on the Pt catalyst, (ii) ionization of the produced hydrogen via diffusion toward the WO$_3$ particles, (iii) diffusion of protons and electrons into the WO$_3$ structure, which is driven by the concentration gradient, and

(iv) excitation of electrons trapped in the d-orbital of W and WO_3 by visible light, leading to a blue color. Consequently, Pt/WO_3 allows a rapid and inexpensive detection of the leakage of the colorless and odorless hydrogen gas by the naked eye. Moreover, as no electricity is used, we can determine the presence of hydrogen using the color change even after a power failure. Therefore, Pt/WO_3 is a promising material for fabricating hydrogen sensors.

However, Pt/WO_3 nanoparticles cannot be handled easily when they are used by themselves. Consequently, they have been utilized in the form of metal oxide thin films on the surfaces of heat-resistant substrates, such as glass [5,6] and alumina [7]. This is because the conventional preparation of the Pt/WO_3 nanoparticles involves a heating process at 700–800 K. However, as these substrates are not flexible, they cannot be easily attached to transportation pipes and storage tanks with complicated shapes. Recently, flexible polymers have been used as substrate materials for the fabrication of Pt/WO_3 particle thin films under mild conditions using a sol-gel method [8–12]. Although methods for synthesizing WO_3 particles under mild conditions have already been reported (e.g., a hydrothermal method at 350 K [13]), the sol-gel process can synthesize WO_3 nanoparticles and simultaneously load the Pt catalyst, producing a large number of nanoparticles compared with hydrothermal methods. Furthermore, the Pt/WO_3 particles prepared using the sol-gel method possess a mixture of crystalline and amorphous phases, which has the advantage of the easy penetration of the particles by hydrogen, thereby shortening the time required for color change. Additionally, crystallinity can be conveniently controlled using the heat treatment conditions of the particles. For both previous and sol-gel methods, Pt/WO_3 layers were formed on the substrate materials after the substrates had already been produced. In addition, there is a lack of studies on the aging degradation of Pt/WO_3 layers on the substrate surfaces.

In this study, a novel fabrication process of hydrogen sensor based on Pt/WO_3 nanoparticles and a polymer is proposed. In this process, instead of forming Pt/WO_3 layers on the surface of existing substrates, Pt/WO_3 particles are prepared in advance and are then incorporated into a polymer membrane synthesis process. Accordingly, we can use flexible polymer materials without concerns about temperatures when fabricating Pt/WO_3. The Pt/WO_3 nanoparticles, prepared in advance, were dispersed in a precursor solution to synthesize a polymer substrate and obtain a Pt/WO_3 nanoparticle-dispersed membrane. The Pt/WO_3 nanoparticles exist not only on the surface but are also distributed and exhibit a color change throughout the material. They are expected to be resistant to aging degradations, such as abrasion. Polydimethylsiloxane (PDMS) membrane, which is transparent, flexible, and gas-permeable, was selected as the polymer. Because of its characteristics, PDMS membranes have been applied in many research fields [14–19]. Here, the optimum heat treatment temperature, content, and crystal structure of Pt/WO_3 nanoparticles have been investigated. Finally, a novel flexible, transparent, resistant, and cost-efficient hydrogen gas leakage membrane sensor was developed to benefit from the rapid and reversible gasochromism of Pt/WO_3 nanoparticles to H_2 gas.

2. Materials and Methods

2.1. Materials

Tungsten hexachloride (WCl_6) and hydrogen hexachloroplatinate hexahydrate ($H_2PtCl_6 \cdot 6H_2O$) for the $PtWO_3$ nanoparticles were purchased from Kanto Chemical Co., Inc. (Tokyo, Japan) and Kishida Chemical Co., Ltd. (Osaka, Japan), respectively. Ethanol was purchased from Kanto Chemical Co., Inc. (Tokyo, Japan). Tertiary butyl alcohol was purchased from Wako Pure Chemical Industries, Ltd. (Osaka, Japan). Sylgard® 184 silicone elastomer kit for the membrane base was purchased from Dow Corning Co. (Midland, MI, USA).

2.2. Synthesis of Pt-Particle-Dispersed Tungsten Trioxide (Pt/WO₃) Nanoparticles

Tungsten hexachloride and hydrogen hexachloroplatinate hexahydrate were first dissolved in ethanol at predetermined atomic ratios (Pt:W = 1:13, 1:100, 1:1000) to form

Pt/WO$_3$ precursor solutions in a dry nitrogen atmosphere. These solutions were then dried in the air at 393 K for 12 h. Next, the dried residues were heated at 473–773 K for 1 h to obtain Pt/WO$_3$ powders. The crystal structures and crystallinities of the obtained powders were characterized using X-ray diffraction (XRD, Ultima IV, Rigaku Corporation, Tokyo, Japan).

2.3. Preparation of Pt/WO$_3$ Nanoparticle-Dispersed Polydimethylsiloxane Membranes

The prepared Pt/WO$_3$ powders were first bead-milled with *t*-butyl alcohol and zirconia beads at 1500 rpm for 1 h. The obtained suspensions were then centrifuged twice at 4800 rpm for 30 min to prepare Pt/WO$_3$ nanoparticle dispersions. These dispersions were added to Sylgard® 184 base at concentrations ranging from 0.50 to 3.00 wt.% and stirred at 393 K and 200 rpm to prepare Pt/WO$_3$ nanoparticle-dispersed bases. Finally, a curing agent (Sylgard® 184 Silicone Elastomer Curing Agent, Dow Corning, Midland, MI, USA) was added to the bases at 10 wt.%. The mixtures were subsequently degassed for 30 min and heated at 353 K for 2 h to obtain Pt/WO$_3$ nanoparticle-dispersed PDMS membranes.

2.4. Evaluation of Hydrogen Gas Response of Pt/WO$_3$ Composite Membranes

The optical response of the Pt/WO$_3$ nanoparticle-dispersed PDMS membranes to hydrogen gas was evaluated using ultraviolet-visible spectroscopy (UV-630, Jasco, Tokyo, Japan). The prepared membranes were placed in a transparent acrylic cell (Figure 1). Baseline correction was performed using an empty cell. The transmission spectrum of the membranes was measured from 400 to 1100 nm by exposing one side of the membrane to synthetic air or 100% H$_2$ gas. The absorbance at 800 nm was measured to evaluate their hydrogen gas-sensing performance. A PDMS membrane containing Pt/WO$_3$ nanoparticles (0.75 wt.% of Pt:W = 1:13) heat treated at 573 K was used for low-concentration H$_2$ gas detection (H$_2$ was diluted with synthetic air). The absorbance was normalized as follows:

$$\Delta \text{Abs} = \text{Abs} - \text{Abs}_0 \tag{1}$$

where Abs and Abs$_0$ are the absorbances at time *t* and 0 s, respectively. The value of *t* ranged from 0 to 600 s. The color difference, transmittance change (ΔT), was calculated as follows:

$$\Delta \text{T} = \text{transmittance in air at 800 nm} - \text{transmittance in H}_2 \text{ at 800 nm} \tag{2}$$
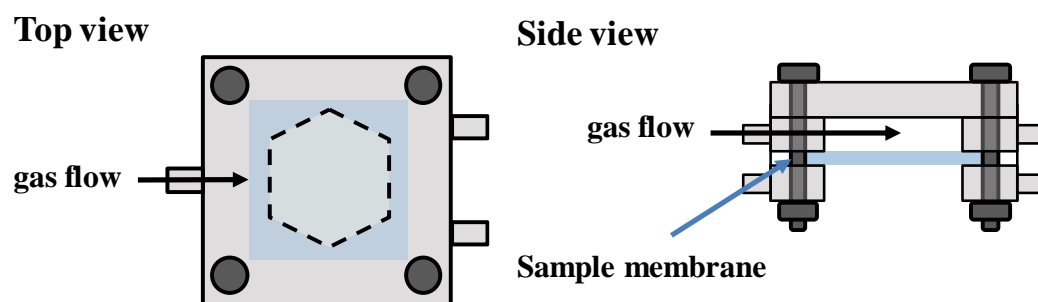

Figure 1. Experimental apparatus for evaluating H$_2$ gas response of membranes.

3. Results and Discussion

3.1. Effect of Compositional Ratio of Platinum and Tungsten Trioxide

The XRD analysis results for the powders with different amounts of Pt are shown in Figure 2. All powders were dried at 393 K and calcined at 673 K for 1 h. The diffraction patterns of the powders correspond to the peaks of monoclinic WO$_3$ (ICDD 01-072-0677) and orthorhombic WO$_3$ (ICDD 01-071-0131). Focusing on the diffraction peak around 29°, the shoulder was observed at higher angle. This was attributed to monoclinic phase as shown in the reference. In contrast, the broad peaks were observed around 44°. These

peaks were attributed to orthorhombic phase. No difference in crystallinity was observed between the samples. The diffraction pattern of Pt (ICDD 00-004-0802) is present only in the diffractogram of the Pt:W = 1:13 powder sample. Therefore, the prepared Pt/WO$_3$ powders were a mixed phase of monoclinic and orthorhombic crystals. The crystallinity did not depend on the amount of loaded Pt.
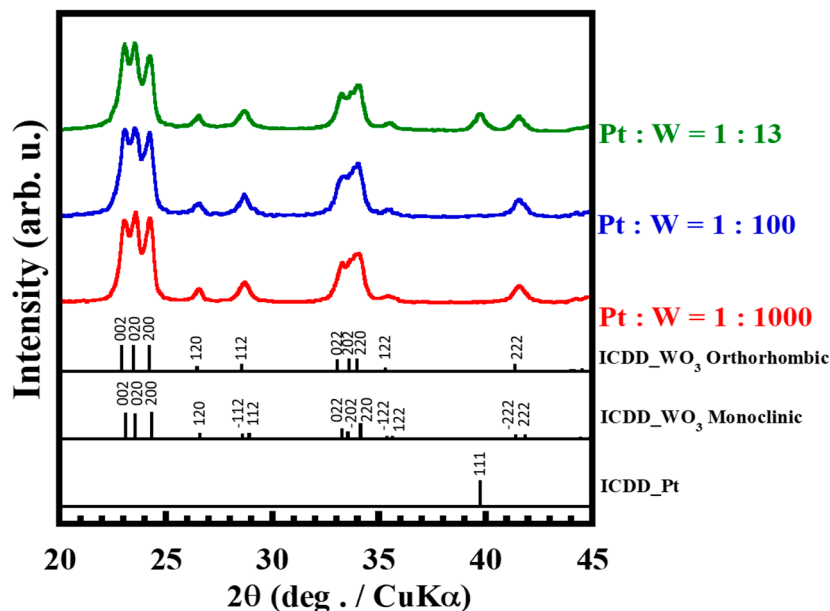

Figure 2. XRD spectra of Pt/WO$_3$ nanoparticles with different amounts of the Pt catalyst.

A photograph of the membranes prepared using the powders under atmospheric conditions is shown in Figure 3a. The Pt/WO$_3$ particle content of the membranes was 0.75 wt.%. Both sample membranes were transparent. A slight coloration was observed in the sample with higher Pt loading (Pt:W = 1:13). This originates from the presence of Pt black. The sizes of Pt particles impregnated on Pt/WO$_3$ prepared by the sol-gel method have been reported to be approximately 5–20 nm, which correspond to those of Pt black [5]. The particle sizes of WO$_3$ in the Pt:W = 1:13 and Pt:W = 1:100 powder samples were 41.0 $\pm$ 7.2 nm and 46.2 $\pm$ 6.3 nm, respectively (Figure S1 in Supplementary Materials). These results agree well with our previous report [20].
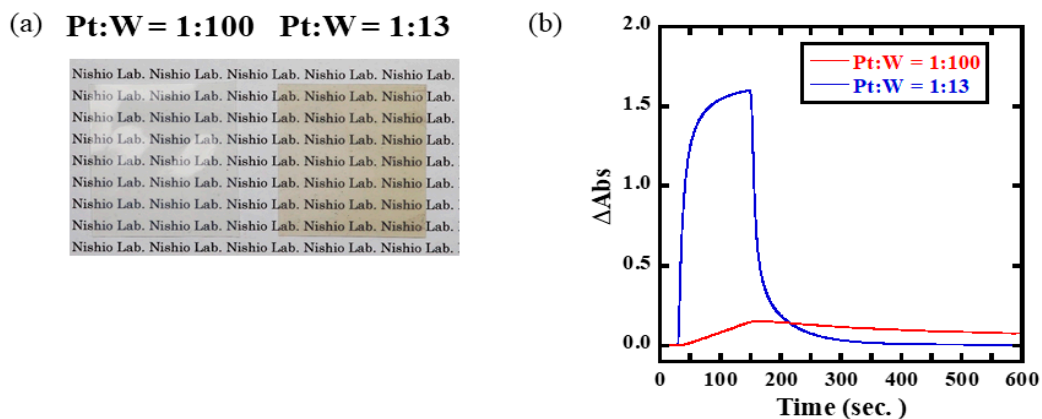

Figure 3. Dependence of H$_2$ response on the amount of the Pt catalyst in Pt/WO$_3$ nanoparticles. (**a**) Typical image of Pt/WO$_3$ nanoparticle-dispersed membranes. (**b**) H$_2$ response measured at 800 nm.

The transmission spectra of the sample membranes and time variation of the absorbance after exposure to 100% H$_2$ gas are shown in Figure S2 and Figure 3b, respectively. The membrane with the higher Pt loading (Pt:W = 1:13) exhibited a faster response to H$_2$ gas than the one with a lower Pt loading (Pt:W = 1:100). This is because the higher loading in the former provides a higher probability of the Pt contact with hydrogen molecules, which results in the faster atomization of hydrogen molecules. Considering these results, the Pt/WO$_3$ membrane with the higher loading of Pt nanoparticles (Pt:W = 1:13) was selected for subsequent experiments.

3.2. Optimization of Pt/WO$_3$ Nanoparticle Content

Photographs of the membranes containing 0.00–3.00 wt.% of Pt/WO$_3$ under ambient conditions are shown in Figure 4a. Pt/WO$_3$ particles were prepared by calcining the Pt:W = 1:13 powder at 673 K. The transparency decreased, and the color changed to dark brown as the number of particles dispersed in the membranes increased. Transmittance at 800 nm is shown in Figure S3a (Supplementary Materials).
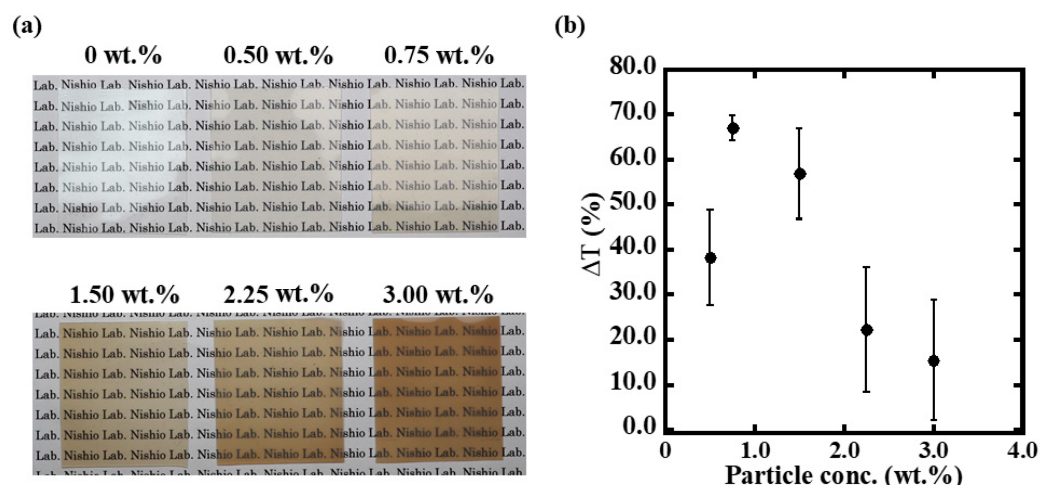

Figure 4. Dependence of transparency and H$_2$ response on the percentage content of Pt/WO$_3$ nanoparticles. (**a**) Typical images of sample membranes. (**b**) Transmittance change when the films were exposed to 100% H$_2$ gas measured at 800 nm.

To investigate the effect of hydrogen gas coloration on the number of dispersed particles, the transmission spectra of membranes exposed to synthetic air and 100% H$_2$ gas are shown in Figure S3b (Supplementary Materials). The color difference response to H$_2$ gas reached the local maximum value of 67.0 ± 2.7% in the 0.75 wt.% Pt/WO$_3$ membrane and decreased at higher particle contents. The 0.75 wt.% Pt/WO$_3$ membrane showed high transparency over a wide wavelength range. The color difference at 800 nm is plotted in Figure 4b. The 0.75 wt.% Pt/WO$_3$ membrane showed the largest transmittance change at 800 nm while there was a sufficient amount of Pt particles for coloring. Considering its applicability for naked-eye hydrogen gas leakage detection, 0.75 wt.% Pt/WO$_3$ was selected as the particle content for the subsequent experiments.

3.3. Optimization of Heat Treatment Temperature on Hydrogen Gas Response Time

The XRD patterns of Pt/WO$_3$ powder samples, for which the precursor solution was dried at 393 K and then heat treated at 573–773 K for 1 h, are shown in Figure 5a. The Pt:W atomic ratio of the samples was set to 1:13. The diffraction peak assigned to WO$_3$ in the 573 K sample was located at approximately 23°. The diffraction intensity increased with heat treatment temperatures. This is due to the improvement in crystallinity of WO$_3$ and grain growth at higher temperatures, as shown in Figure S1 (Supplementary Materials). Moreover, multiple diffraction peaks were observed at higher treatment temperatures. Depending on the heat treatment temperature, WO$_3$ can exist stably in various forms

at room temperature, including monoclinic, triclinic, hexagonal, orthorhombic, or cubic systems. The intensity ratios of 022, 202, and 220 planes at approximately $23°$ were different for the three treatment temperatures. Compared to the International Centre for Diffraction Data cards (01-071-0131, 01-072-0677), the prepared Pt/WO_3 powders seemed to be mixtures of monoclinic and orthorhombic phases for treatment temperatures up to 773 K. At higher temperatures, the diffraction intensity increased and the full width at half maximum of the peak at approximately $40°$ (derived from the Pt 111 plane) decreased. This decrease is due to the grain growth in Pt particles induced by the heat treatment at high temperatures. The crystallite sizes of Pt treated at 673 and 773 K, for which clear peaks were observed, were estimated using Scherrer's equation. In the calculations, the peaks of the 111 plane were used for Pt. Based on Langford and Wilson's empirical rule, the Scherrer's constant was selected as a spherical approximation for WO_3 and a cubic approximation for Pt [21]. The crystallite sizes of Pt at 673 and 773 K were 1.09 and 1.32 nm, respectively. These results indicate that the grain growth of Pt also occurred as the heat treatment temperature increased.
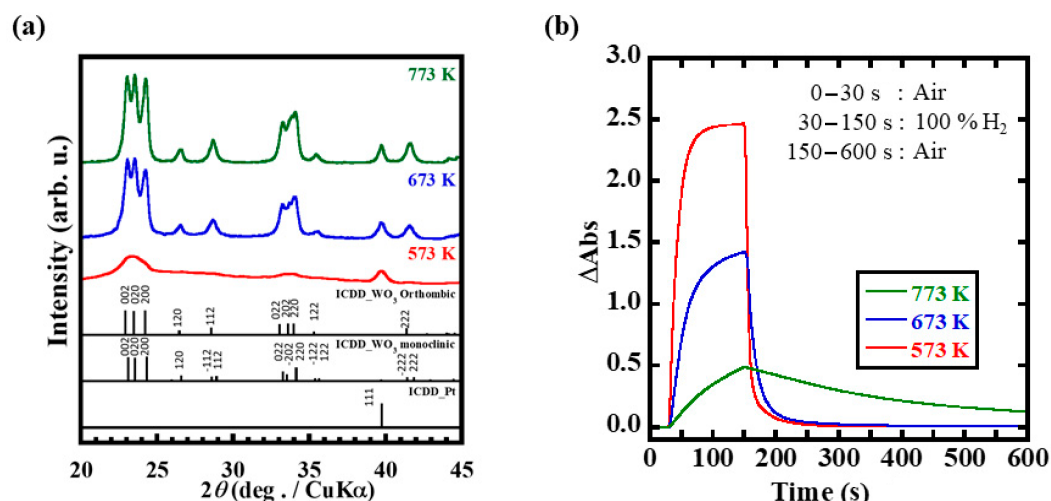

Figure 5. Dependence of H_2 response on the Pt/WO_3 nanoparticle heat treatment temperature. (**a**) Pt/WO_3 powder XRD spectra. (**b**) H_2 response measured at 800 nm.

The transmittance and color changes of the Pt/WO_3 powder samples heat treated at 573–773 K for 1 h are shown in Figures S4a and S5b (Supplementary Materials). The maximum color change was observed in the dispersed membrane prepared via heat treatment at 573 K, followed by the membranes treated at 673 and 773 K. The degree of color change at 473 K was smaller than that at 673 K (data not shown). In addition, the coloring reactions of the films dispersed with the 573 K and 673 K heat-treated powders saturated but did not reach saturation in the membrane dispersed with the 773 K heat treated powder. The maximum coloring rate was obtained for the film dispersed with the 573 K heat-treated powder (Figure S4b in Supplementary Materials). These results indicate that the optimal heat treatment condition for Pt/WO_3 dispersed in the PDMS film with respect to the gasochromic reaction performance when hydrogen gas was 573 K. At this temperature, a WO_3 crystal structure with coloring sites could be formed while retaining a large accessible surface area.

3.4. Hydrogen Gas Detection Performance of Pt/WO3 Composite Membranes

The H_2 gas detection performance of the Pt/WO_3 composite membrane is shown in Figure 6. The absorption was instantly saturated for 100% H_2 gas, but for hydrogen concentrations less than 1.0%, the absorption did not saturate. The concentration gradient is the driving force for gas diffusion in the membrane. The opposite surface, which served as the target for the hydrogen gas flow, was exposed to the atmosphere, and the decolorization reaction occurred through the diffusion of oxygen from the atmosphere. Therefore, the

color of the film is determined by the balance between the coloring and decoloring reactions. The latter was predominant at low hydrogen concentrations, which resulted in the absence of transmittance changes. Because 10% of ΔT is sufficient to determine the color change with the naked eye, the lower limit of detection was defined as 10%, and the concentration was 0.4%. Because hydrogen gas becomes explosive when its concentration exceeds 4% in the atmosphere, the lower limit of detection is one-tenth of the concentration, and the ability to detect hydrogen gas is sufficient for practical applications.
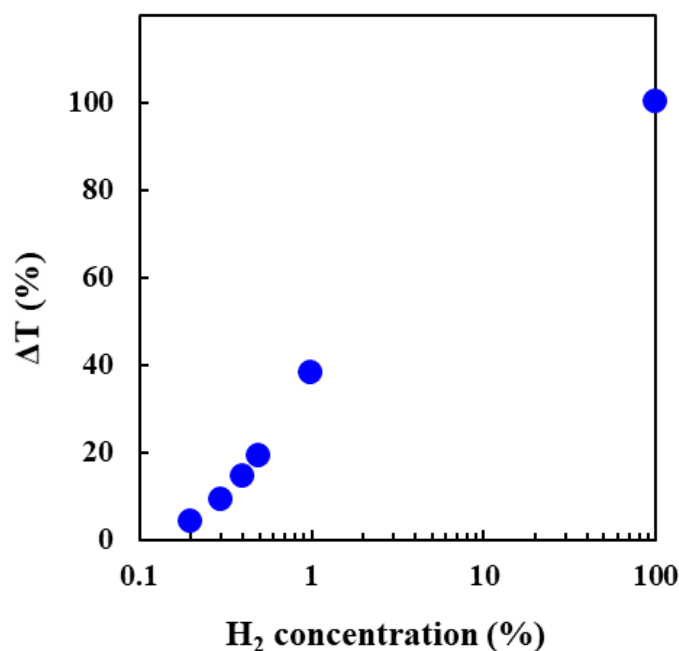

Figure 6. H_2 gas detection performance of the Pt/WO$_3$ composite membrane. (Pt:W = 1:13; heat treatment at 573 K; particle concentration of 0.75 wt.%; measurement wavelength of 800 nm; exposure to H_2 gas concentrations of 0.1–100 vol%).

As shown in Figure 7, the Pt/WO$_3$ composite membrane is transparent and flexible. It can be easily attached to various shapes for practical applications. Using this membrane, the detection of hydrogen gas is qualitative, but the existence can be determined with the naked eye without the use of electricity. The Pt/WO$_3$ nanoparticles exist not only on the surface of the membrane but are also distributed and exhibit a color change throughout the membrane. Therefore, they are expected to be resistant to aging degradations. The effect of humidity on Pt/WO$_3$ coloration was verified in a previous study [22]. In this study, PDMS is a hydrophobic polymer, which prevents water from diffusing into the membrane, and the effect of humidity is considered to be small. However, water molecules are also generated during Pt catalysis in the decoloration step. This is because the oxygen molecules react with hydrogen in WO$_3$ to return to the transparent state. The interference of the generated H_2O on hydrogen gas sensing can be removed by heating the sensor over 353 K. For practical applications, the evaluation of the durability of repeated coloration/decoloration cycles might be needed in future.
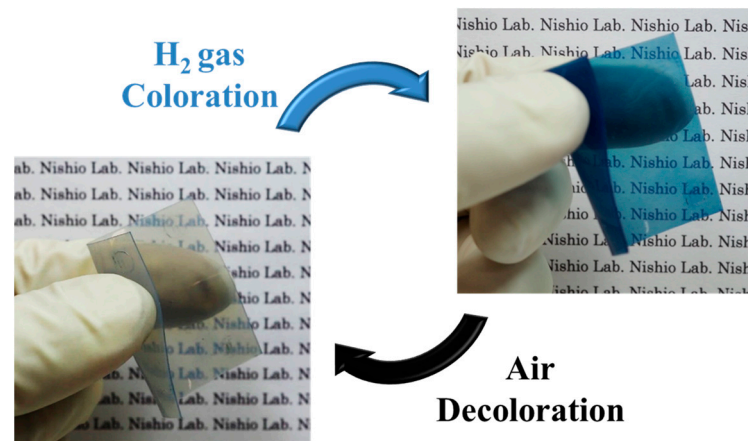
Figure 7. Hydrogen gas responsivity, transparency, and flexibility of the Pt/WO$_3$ particle-containing membrane. (Pt:W = 1:13; heat treatment at 573 K; particle concentration of 0.75 wt.%; exposed to the H$_2$ gas concentration of 100%).

4. Conclusions

Flexible and transparent Pt/WO$_3$ nanoparticle-dispersed membranes toward H$_2$ gas leakage sensor was prepared. First, the effect of the composition ratio of platinum and tungsten oxide was first investigated. The Pt:W = 1:13 membrane was found to be highly transparent and exhibited a sufficient color change in response to the H$_2$ gas. The effects of the Pt/WO$_3$ nanoparticle content in the composite membrane were also investigated. Although a simple trade-off exists between the nanoparticle content and transparency, the latter affects the hydrogen gas detection performance. Therefore, the content was optimized for the color difference. The membrane containing 0.75 wt.% of Pt/WO$_3$ nanoparticles exhibited a local maximum color difference. Subsequently, the effect of heat treatment temperature was investigated. While high-temperature heat treatment increased the crystallinity of the Pt/WO$_3$ nanoparticles, it also decreased the area accessible to hydrogen gas, contributing to a gasochromism reaction because of the grain growth in the particles. Sensitive detection and rapid response to H$_2$ gas were achieved in the membrane dispersed with the 573 K heat-treated nanoparticles. Finally, sufficient visibility to the low concentration of H$_2$ gas (0.4%, which is one-tenth of the minimum explosive concentration) and the flexibility of the membrane were confirmed.

The membrane developed in this study is an inexpensive, safe, and easy-to-use hydrogen gas sensor. Because Pt/WO$_3$ nanoparticles are dispersed in the membrane, resistance to aging degradation and abrasion can be expected. In situations where it is not possible to inspect the H$_2$ gas-detection membrane immediately, it would be desirable for the coloring to remain after the detection of H$_2$ gas. The membrane developed in this study returned to its original transparent color (from the blue color corresponding to the detection of H$_2$ gas) relatively rapidly after it was placed in an air environment. A material that combines the hydrogen gas detection performance with memory properties, without compromising the advantages of the membrane, is a promising development. In future studies, the formation of a double-layer film with a gas barrier on one side or a controlled polymer network structure with selective H$_2$ gas permeation will be investigated as possible solutions for achieving this goal.

when the films were exposed to 100 % H_2 gas measured at 800 nm. The solid lines denote the transmittance in atmospheric air and the dot-ted lines, the transmittance in 100% H_2; Figure S4: Dependence of H_2 response on Pt/WO_3 nanoparticle heat treatment temperature. (a) Transmittance of sample membranes. The solid lines denote the transmittance in atmospheric air and the dotted lines, the transmittance in 100% H_2. (b) Maximum coloring velocity when the films were exposed to 100 % H_2 gas.

Author Contributions: Conceptualization: R.I., Y.Y. and K.N.; Design of the experiments: R.I., Y.M., Y.Y. and K.N.; Experiments conduction and data analysis: R.I., Y.M., Y.Y. and K.N.; Project administration: R.I., Y.Y., K.F. and K.N.; Writing of the manuscript: R.I., Y.M., Y.Y., K.F. and K.N. All authors have read and agreed to the published version of the manuscript.

Institutional Review Board Statement: Not applicable.

Data Availability Statement: Not applicable.

Conflicts of Interest: The authors declare no conflict of interest.

References

1. Sinigaglia, T.; Lewiski, F.; Santos Martins, M.E.; Mairesse Siluk, J.C. Production, storage, fuel stations of hydrogen and its utilization in automotive applications-a review. *Int. J. Hydrogen Energy* **2017**, *42*, 24597–24611. [CrossRef]
2. Kohn, H.W.; Boudart, M. Reaction of Hydrogen with Oxygen Adsorbed on a Platinum Catalyst. *Science* **1964**, *145*, 149–150. [CrossRef]
3. Zhou, X.; Dai, Y.; Liu, F.; Yang, M. Highly Sensitive and Rapid FBG Hydrogen Sensor Using $Pt-WO_3$ with Different Morphologies. *IEEE Sens. J.* **2018**, *18*, 2652–2658. [CrossRef]
4. Castillero, P.; Rico-Gavira, V.; López-Santos, C.; Barranco, A.; Pérez-Dieste, V.; Escudero, C.; Espinós, J.P.; González-Elipe, A.R. Formation of Subsurface W^{5+} Species in Gasochromic Pt/WO_3 Thin Films Exposed to Hydrogen. *J. Phys. Chem. C* **2017**, *121*, 15719–15727. [CrossRef]
5. Yamaguchi, Y.; Emoto, Y.; Kineri, T.; Fujimoto, M.; Mae, H.; Yasumori, A.; Nishio, K. Hydrogen gas-sensing properties of Pt/WO_3 thin film in various measurement conditions. *Ionics* **2012**, *18*, 449–453. [CrossRef]
6. Hsu, C.-H.; Chang, C.-C.; Tseng, C.-M.; Chan, C.-C.; Chao, W.-H.; Wu, Y.-R.; Wen, M.-H.; Hsieh, Y.-T.; Wang, Y.-C.; Chen, C.-L.; et al. An ultra-fast response gasochromic device for hydrogen gas detection. *Sens. Actuators B Chem.* **2013**, *186*, 193–198. [CrossRef]
7. Ippolito, S.J.; Kandasamy, S.; Kalantar-zadeh, K.; Wlodarski, W. Hydrogen sensing characteristics of WO_3 thin film conductometric sensors activated by Pt and Au catalysts. *Sens. Actuators B Chem.* **2005**, *108*, 154–158. [CrossRef]
8. Yamaguchi, Y.; Imamura, S.; Ito, S.; Nishio, K.; Fujimoto, K. Influence of oxygen gas concentration on hydrogen sensing of Pt/WO_3 thin film prepared by sol–gel process. *Sens. Actuators B Chem.* **2015**, *216*, 394–401. [CrossRef]
9. Okazaki, S.; Johjima, S. Temperature dependence and degradation of gasochromic response behavior in hydrogen sensing with Pt/WO_3 thin film. *Thin Solid Film.* **2014**, *558*, 411–415. [CrossRef]
10. Deptula, A.; Olczak, W.L.T.; Sartowska, B.; Giorgi, L.; Moreno, A.; di Bartolomeo, A. Preparation of Pt/WO_3 Powders and Thin Films on Porous Carbon Black and Metal Supports by the Complex Sol-Gel Process. *J. New Mater. Electrochem. Syst.* **2003**, *6*, 71–74.
11. Ishihara, R.; Yamaguchi, Y.; Tanabe, K.; Makino, Y.; Nishio, K. Preparation of Pt/WO_3-coated polydimethylsiloxane membrane for transparent/flexible hydrogen gas sensors. *Mater. Chem. Phys.* **2019**, *226*, 226–229. [CrossRef]
12. Nishizawa, K.; Yamada, Y.; Yoshimura, K. Low-temperature chemical fabrication of $Pt-WO_3$ gasochromic switchable films using UV irradiation. *Sol. Energy Mater. Sol. Cells* **2017**, *170*, 21–26. [CrossRef]
13. Takács, M.; Zámbó, D.; Deák, A.; Pap, A.E.; Dücső, C. WO_3 nano-rods sensitized with noble metal nano-particles for H_2S sensing in the ppb range. *Mater. Res. Bull.* **2016**, *84*, 480–485. [CrossRef]
14. Lee, J.Y.; Park, H.; Lee, J.S.; Yoon, S.; Lee, J.-H. Biphenyl-based covalent triazine framework-incorporated polydimethylsiloxane membranes with high pervaporation performance for n-butanol recovery. *J. Membr. Sci.* **2020**, *598*, 117654. [CrossRef]
15. Zhang, S.Q.; Fouda, A.E.; Matsuura, T. A study of pervaporation of aqueous benzyl alcohol solution by polydimethylsiloxane membrane. *J. Membr. Sci.* **1992**, *70*, 249–255. [CrossRef]
16. Ishihara, R.; Tanabe, K.; Inomata, S.; Matsui, R.; Kitane, R.; Hosokawa, K.; Maeda, M.; Kikuchi, A. Fabrication of Storable Surface-Functionalized Power-Free Microfluidic Chip for Sensitive MicroRNA Detection Utilizing Ultraviolet Grafting. *Ind. Eng. Chem. Res.* **2020**, *59*, 10464–10468. [CrossRef]
17. Ishihara, R.; Katagiri, A.; Nakajima, T.; Matsui, R.; Komatsu, S.; Hosokawa, K.; Maeda, M.; Tomooka, Y.; Kikuchi, A. Design of a surface-functionalized power-free microchip for extracellular vesicle detection utilizing UV grafting. *React. Funct. Polym.* **2019**, *142*, 183–188. [CrossRef]
18. Evenou, F.; Fujii, T.; Sakai, Y. Spontaneous Formation of Highly Functional Three-Dimensional Multilayer from Human Hepatoma Hep G2 Cells Cultured on an Oxygen-Permeable Polydimethylsiloxane Membrane. *Tissue Eng. Part C Methods* **2009**, *16*, 311–318. [CrossRef]

19. Liu, X.; Zhu, Y.; Nomani, M.W.; Wen, X.; Hsia, T.-Y.; Koley, G. A highly sensitive pressure sensor using a Au-patterned polydimethylsiloxane membrane for biosensing applications. *J. Micromech. Microeng.* **2013**, *23*, 025022. [CrossRef]
20. Yamaguchi, Y.; Nemoto, C.; Ito, S.; Nishio, K.; Fujimoto, K. Improvement of hydrogen gas sensing property of the sol–gel derived Pt/WO_3 thin film by Ti-doping. *J. Ceram. Soc. Jpn.* **2015**, *123*, 1102–1105. [CrossRef]
21. Langford, J.I.; Wilson, A.J.C. Scherrer after sixty years: A survey and some new results in the determination of crystallite size. *J. Appl. Crystallogr.* **1978**, *11*, 102–113. [CrossRef]
22. Yamaguchi, Y.; Imamura, S.; Nishio, K.; Fujimoto, K. Influence of temperature and humidity on the electrical sensing of Pt/WO_3 thin film hydrogen gas sensor. *J. Ceram. Soc. Jpn.* **2016**, *124*, 629–633. [CrossRef]